Published in final edited form as:
Cancer. 2011 July 1; 117(13): 2898–2909. doi:10.1002/cncr.25818.

CpG Island Methylation Profiling in Human Salivary Gland Adenoid Cystic Carcinoma:

DNA Methylation in Salivary Gland ACC

Achim Bell, PhD[1], **Diana Bell, MD**[2], **Randal S. Weber, MD**[3], and **Adel K. El-Naggar, MD, PhD**[2]

[1] Department of Pathology and Cancer Institute, The University of Mississippi Medical Center, Jackson, Mississippi

[2] Department of Pathology, The University of Texas M. D. Anderson Cancer Center, Houston, Texas

[3] Department of Head and Neck Surgery, The University of Texas M. D. Anderson Cancer Center, Houston, Texas

Abstract

BACKGROUND—DNA methylation is a fundamental epigenetic event associated with physiologic and pathologic conditions including cancer. Hypermethylation of CpG islands at active gene promoters lead to transcriptional repression while hypomethylation is associated with gene overexpression. The aim of this study was to identify genes in adenoid cystic carcinoma (ACC) of salivary gland strongly deregulated by epigenetic CpG island methylation, to validate selected genes by conventional techniques, and to correlate the findings with clinico-pathologic factors.

METHODS—We analyzed 16 matched normal and tumor tissues for aberrant DNA methylation using the methylated CpG island amplification and microarray (MCAM) method, and the pyrosequencing technique.

RESULTS—Microarray analysis showed hypomethylation in seven, and hypermethylation in 32 CpG islands. Hypomethylation was identified in CpG islands near FBXO17, PHKG1, LOXL1, DOCK1 and PARVG. Hypermethylation was identified near genes encoding predominantly transcription factors (EN1, FOXE1, GBX2, FOXL2, TBX4, MEIS1, LBX2, NR2F2, POU3F3, IRX3, TFAP2C, NKX2-4, PITX1, NKX2-5), and 13 genes with different functions (MT1H, EPHX3, AQPEP, BCL2L11, SLC35D3, S1PR5, PNLIPRP1, CLIC6, RASAL, XRN2, GSTM5, FNDC1, INSRR). Four CpG islands by EN1, FOXE1, TBX4, and PITX1 were validated by pyrosequencing.

CONCLUSION—The highly methylated genes in tumor versus normal are linked to developmental, apoptotic and other fundamental cellular pathways, suggesting that downregulation of these genes is associated with ACC development and progression. With EN1 hypermethylation showing potential as possible biomarker for ACC in salivary gland, the biological and therapeutic implications of our findings require further preclinical investigations.

Keywords

adenoid cystic carcinoma; epigenetics; CpG island methylation; MCAM; pyrosequencing

The first two authors contributed equally to this article.

The authors have no conflicts of interest to disclose.

BACKGROUND

Salivary gland tumors comprise histopathologically and clinically diverse entities of disputed histogenesis and unpredictable behavior. Approximately 40% of these tumors are malignant, and represent 5% of all head and neck carcinomas. Complete surgical excision with and without post-operative radiotherapy is the primary treatment of these patients. Adenoid cystic carcinoma (ACC), the second most frequent malignancy of the major and minor salivary glands, comprise of approximately 15–23% of all carcinomas at these locations. Despite thorough resection, up to 60% of patients experience locoregional or distant metastases. The median survival in the presence of distant metastases is around three years, though surprisingly, up to 10% of these patients may survive 10 years or longer with their metastases. Extensive efforts to characterize molecular events associated with these tumors are being done to identify biomarkers for prognostication and therapy assessment.

Epigenetic modifications may play a role in the development of these tumors. Methylation plays an important role in the transcriptional inactivation of tumor suppressor genes in human cancer. CpG islands have been defined as genomic regions with a minimum of 200 bp, with % G+C greater than 50 and with observed/expected CpG ratio above 60%. More recently [1], studies have further defined CpG island sas regions of DNA greater than 500 bp with a G+C equal to or greater than 55% and observed CpG/expected CpG ratio of 0.65. In actively transcribed genes the CpG sites in CpG islands of promoter regions are unmethylated, whereas increased cytosine methylation in the island CpG sites is associated with reduced gene expression and possible gene silencing.

CpG methylation has been reported to play an important fundamental role in a large spectrum of biological processes including aging, infectious diseases, and cancer. The availability of molecular techniques to evaluate the methylation status of CpG islands in cancer related genes has allowed for the evaluation of CpG methylation in tissue specimens of both archival and frozen states. CpG hypermethylation is critical for silencing the expression of certain tumor suppressor genes, and globally by regulating differentiation programs in many tumor types. The levels of CpG methylation have thus been used to subclassify tumors, predict response to chemotherapeutic agents that are metabolized or antagonized by cellular enzymes regulated by promoter methylation, and to assess the effects of methylating and demethylating therapies.

The aim of this study was (1) to identify differentially methylated target genes in ACC, and (2) to validate and investigate selected genes.

METHODS & MATERIALS

Tissue samples

Fresh tissues from 16 patients (ACC tumors and matching normal salivary tissue peripheral to the neoplasm) were obtained from patients surgically treated at the Department of Head and Neck Surgery (MD Anderson Cancer Center, Houston, TX, USA) using appropriate written informed consent obtained after approval by the MDACC Institutional Review Board. The quality of all specimens harvested was evaluated for tumor content and quality issue in frozen sections and tumor specimens containing at least 85% tumor cells.

DNA extraction

Genomic DNA was extracted from freshly frozen tissues using QIAamp DNA Micro Kit (Qiagen) according to the manufacturer’s protocol.

Methylated CpG island amplification (MCA)

The procedure was performed according to Toyota et al. [2]. In brief, 5 μg of DNA was digested with 100 units of SmaI for 16 h (all restriction enzymes were from New England Biolabs), followed by digestion with 20 units of XmaI for 6 h. The fragmented DNA was precipitated with ethanol. RXMA PCR adaptors were prepared by incubation of the oligonucleotides RXMA24 (5′-AGCACTCTCCAGCCTCTCACCGAC-3′) and RXMA12 (5′-CCGGGTCGGTGA-3′ for 2 min at 65°C, followed by cooling to room temperature for 1 h. The XmaI-DNA fragments (0.5 μg) were ligated to 0.5 nmol of RXMA adaptors using T4 DNA ligase (New England Biolabs). PCR was performed using 3 μL each of the ligation mix as template in a 100 μL volume containing 100 pmol of RXMA24, 5 units of Taq DNA polymerase, 67 mM Tris-HCl (pH 8.8), 4 mM $MgCl_2$, 16 mM $NH_4(SO_4)_2$, and 10 μg/mL BSA. In a thermal cycler the reaction mixture was incubated for 5 min at 72°C and for 3 min at 95°C. Samples were subjected to 20 cycles of amplification consisting of 1 min at 95°C and 3 min at 72°C. The final extension was 10 min at 72°C. 10 μL of PCR product was resolved in 1.5% agarose gel and visualized under UV after ethidium bromide staining. Successful MCA reactions resulted in amplicon smear ranging from 300 bp to 3 kb, with most amplicons at 1 kb. PCR products were purified using the PCR purification kit from Qiagen.

Methylated CpG island microarray

Incorporation of amino-allyl dUTP (aa-dUTP; Sigma) into 600 ng each of tumor DNA and normal DNA was conducted using the Bioprime DNA-labeling system protocol (Life Technologies) [3]. Cy5 and Cy3 fluorescent dyes were coupled to aa-dUTP-labeled tumor and normal DNA, respectively, and cohybridized to Agilent 4×44k custom CGH microarray slides. The array included 42222 probes corresponding to 9008 autosomal genes. The probes were selected to recognize Sma I/Xma I restriction fragments from regions close to gene transcriptional start sites (TSS) [4].

Microarray protocols including the hybridization and post-hybridization procedures were performed according to De Risi et al [5]. Hybridized slides were scanned with the GenePix 4000A scanner (Axon), and the acquired images were analyzed with the software GenePix Pro 3.0. Two-step global lowest normalization was done using the background-subtracted median intensity of each spot, and the resultant log2 ratios were averaged from duplicate experiments (except for primary tumors, where only one array experiment was available per sample). Based on published expression microarray methods, CpG island tags having a Cy5/Cy3 log2 ratios ≥1.3 (2.5-fold enrichment) were considered hypermethylation-specific signals. Accordingly Cy3/Cy5 log2 ratios ≥ 1.3 were considered cut off for hypomethylation [4]. This log2 ratio value was also supported by our pyrosequencing validation experiments as the best cutoff to achieve optimal sensitivity and specificity, since lower values show high variance in CpG-methylation of tumor compared to normal tissue.

Pyrosequencing

Validation of the methylation status of the 4 selected genes (EN1, FOXE1, TBX4, and PITX1) was performed using pyrosequencing based methylation analysis. All primers for pyrosequencing were designed using the Pyrosequencing Assay Design 2.0 software (Qiagen/Biotage). Genomic DNA (2 μg) was modified with sodium bisulfite using an EpiTect Bisulfite Kit (Qiagen). For each gene, a 50 μL PCR was carried out in 60 mM Tris-HCl (pH 8.5), 15 mM ammonium sulfate, 2 mM $MgCl_2$, 10% DMSO, 1 mM dNTP mix, 1 unit of Taq polymerase, 5 pmol of the forward primer, 2 pmol of the reverse primer, and 50 ng of bisulfite modified genomic DNA. For pyrosequencing, 4.5 pmol of biotinylated universal primer (5′-GGGACACCGCTGATCGTTTA-3′) was added to the PCR reactions. The forward primer has a 23 bp linker sequence on the 5′-end that is recognized by a biotin-

labeled primer so that the final PCR product can be purified using Sepharose beads. PCR cycling conditions were 30 sec at 95°C, 30 sec at 50° –57°C, and 30 sec at 72°C for 50 cycles. The biotinylated PCR product was purified and denatured into single strands to act as a template in a pyrosequencing reaction using the Pyrosequencing Vacuum Prep Tool (Pyrosequencing, Inc.) according to manufacturer's protocol. In brief, the PCR product was bound to Streptavidin-Sepharose HP (Amersham Biosciences), and the Sepharose beads containing the immobilized PCR product were purified, washed, denatured using a 0.2 M NaOH solution, and washed again. 0.3 μM pyrosequencing primer (sequence-specific to each gene) was annealed to the purified single-stranded PCR product, and pyrosequencing was performed using the PSQ HS 96 Pyrosequencing System (Qiagen). Methylation quantification was performed using the provided PyroQ-CpG software. The program calculates for each single CpG dinucleotide the ratio between its methylated and non-methylated form resulting in percentage of methylation. The methylation degree of each CpG island area was then determined by calculating the average of the methylation differences of all CpG sites analyzed in each gene region.

Data analysis

Highly differentially methylated CpG islands by MCAM analysis with consistent changes in all 16 ACC tumors were determined as follows: for each microarray probe the log2 of the average signal ratios over all 16 patients minus average deviation was calculated for hyper- and for hypomethylation. Only log2 ratio averages of all 16 patients which yielded values ≥1.3 were considered significant, showing high differences in CpG methylation and were used for further analysis. For all significant log2 probes the annotations available for this microarray platform from Agilent were validated or corrected using the UCSC Genome Browser.

Then all significant log2 probe values were arranged in groups according to their location in CpG islands and associated genes. These significant log2 probe values were averaged for each associated gene region, and the results are presented in two ranking tables for differential CpG methylation sorted for highest hyper- and hypomethylation and lowest variation over all patients (tables 1 and 2).

In the second step, the significantly hypermethylated genes were analyzed for cross tumor comparison. For this, for each tumor from individual patients the average log2 ratios were calculated for all probes in each of the significantly hypermethylated gene regions determined in the previous step. The resulting hypermethylation log2 values from individual tumors were then sorted in increasing order for each significantly hypermethylated gene region. These results were used to create trend lines showing individual tumors arranged in the order of increasing hypermethylation. The trend lines were compared with the patient's clinico-pathological parameters to test them for correlation and thus whether they have potential as diagnostic markers.

RESULTS

Clinical and pathological data

Of the 16 patients with ACC, 9 were female and 7 were male who ranged in age from 37 to 85 years (mean, 57.6 years) at the time of diagnosis. Five tumors arose from the maxilla and hard palate, three tumors in the parotid, two from base of tongue, two from floor of mouth, and one each from submandibular gland, retromolar trigone, pharynx and the lip. The tumors ranged from 1.0 to 6.5 cm in diameter (mean, 3.0 cm), and 31 % of patients (5 of 16) developed distant metastases. All patients were treated primarily with surgery, and 14 (88%) also received adjuvant radiotherapy. Only 3 patients received postoperative chemotherapy.

At the last follow-up (mean follow-up, 51 months; range, 7–240 months), 13 patients (81%) were alive (table 3).

MCAM analysis

In order to identify methylated targets in ACC, we generated PCR amplicons from 16 ACC tumors using the methylated CpG island amplification (MCA) protocol [2]. Control amplicons were obtained from normal matched tissues. The generation of MCA amplicons depends on the presence of two SmaI restriction sites in relatively close proximity (no more than 1 – 2 kb apart), which occurs in ~80% of the promoter CpG islands as calculated from in silico digestion of the human genome. This leaves an estimated amount of 6180 probes for investigation under our experimental conditions [4]. Amplicons from tumors and controls were labeled with Cy5 dye, and Cy3 respectively. Equimolar aliquots of tumor and normal labeled amplicons were cohybridized to a microarray chip containing Agilent 4×44k custom CGH microarray slides. The slides included 42222 probes corresponding to 9008 autosomal genes. Duplicate experiments were performed for each tumor, and the results were averaged for data analysis. Hypermethylated genes in tumor specimens were visualized as red spots, and normalized log2 ratio values of ≥1.3 (equivalent to ~2.5-fold tumor/normal signal intensity) were used as a cutoff for hypermethylation. By comparing probe intensity for each tumor to normal controls, significant differential intensity difference can be detected in tumors. A total of 82 probes corresponding to 32 CpG islands were identified to be significantly hypermethylated in the ACC tumors.

The comparison between the 16 matching normal tissues shows no significant difference in methylation. This shows a low rate of technical artifacts, and that tissue-specific methylation differences in normal tissues are rare, as has been shown before [6]. It further supports the findings that the differences in ACCs represent cancer-relevant methylation rather than normal tissue-specific methylation differences.

Identification of new methylated genes in ACC using MCAM

The 82 probes found to be significantly hypermethylated were annotated using the microarray platform of Agilent and the UCSC Genome Browser. Among the annotated loci, 32 were representative of CpG island regions. Some genome loci correspond to two genes (bidirectional promoter), and others were represented more than once (replicated probes), resulting in a total of 34 associated genes.

Tables 1 & 2 show hyper- and hypomethylated genes variable log2 ratios between ACC and normal tissue: 1.3 to 2.3 fold increase in hypermethylation for 32 associated gene regions, and 1.3 to 1.5 fold changes in hypomethylation for only 7 associated genes.

Significant hypermethylation were found at the TSS (transcriptional start site) of genes which encode for transcription factors, mainly homeobox genes: EN1, GBX2, MEIS1, LBX2, POU3F3, IRX3, NKX2-4, PITX1, NKX2-5, forkhead box genes: FOXE1, FOXL1, and other transcription factors: TBX4, NR2F2, TFAP2C. Significant hypermethylations furthermore occur in 13 other regions associated with genes of different functions: MT1H (cellular processes on binding, storage, and transport of Zn/metal ions), EPHX3 (epoxide hydrolase 3, removal of mutagenic epoxides), AQPEP (laeverin, membrane metallopeptidase, protein catabolism), BCL2L11 (apoptotic activator), SLC35D3 (carbohydrate transport), S1PR5 (receptor involved in endothelial differentiation), PNLIPRP1 (lipid catabolism), CLIC6 (chloride channel protein), RASAL (Ras GTPase activator), XRN2 (RNA metabolism), GSTM5 (glutathione transferase), FNDC1 (desmoplastic response), INSRR (insulin receptor related kinase), and 6 genes of unknown

functions: C21orf91, MEGF11, KLHDC7B, SLFN13, FAM176B, C1orf113, and one pseudogene: MT1IP.

Significant hypomethylation was noted at sites near the TSS of FBXO17 (ubiquitination, protein catabolism), PHKG1 (serine/threonine protein kinase, glycogen catabolism), and LOXL1 (extracellular amine oxidase), DOCK1 (cell surface extension), PARVG (cell adhesion), and the unknown genes C19orf24, C15orf38.

Pyrosequencing for MCAM validation

To evaluate the reproducibility of our MCAM results, a set of the four genes EN1, FOXE1, TBX4, and PITX1, which was analyzed as hypermethylated with MCAM, was selected for validation by pyrosequencing. All CpG sites tested were strongly methylated in ACCs, and showed low-to-absent methylation in normal matched DNA, (see fig. 1 as an example for pyrosequencing in the EN1 promoter region). The methylation data are presented as the average methylation across all tumors of each CpG site analyzed by pyrosequencing (fig. 2). For each gene region an average methylation difference between normal and tumor tissues was calculated from all pyrosequenced CpG sites, yielding for EN1: 59%, FOXE1: 53%, TBX4: 43%, and PITX1: 53%. This resulted in an average overall methylation difference of 52% +/− 9. Thus all gene regions analyzed by pyrosequencing showed DNA hypermethylations (fig. 2) as first detected by MCAM.

Classification of ACCs into clinical subgroups using MCAM

Significantly hypermethylated 32 CpG island regions were further tested for differences across tumors. This identified three distinctive patterns of tumors showing either low, moderate or very high hypermethylations in almost all 32 gene regions.

Comparing the methylation status of these 32 genome loci with the clinical and pathological parameters of the patients yielded the EN1 hypermethylated gene promoter as the best fit. The EN1 promoter hypermethylation showed between tumors the highest differences in hypermethylation, but low variation in hypermethylation for all 9 different MCAM probes located in the CpG island of the EN1 promoter (fig. 3). The extent of the EN1 promoter hypermethylation was significantly correlated with clinical parameters including histological grading of tumor, location of tumor and final outcome of patient (fig. 4). Based on the degree of the hypermethylation of the EN1 promoter the 16 adenoid cystic carcinoma tumors can be sub-classified in 3 patient subgroups: group 1 (log2 ratio <2.2), group 2 (log2 ratio 2.2–4.5), and group 3 (log2 ratio >4.5).

With this EN1 categorization the patients' clinico-pathological findings present as follows: In group 1 (#7, 8), one of the patients had a history of prior parotidectomy for a benign mixed tumor in 1999 (per outside clinical notes), with the ACC cribriform type found in the parotid bed (#7), and the other tumor was a cribriform type of lip primary origin (#8). Group 2 included twelve patients: three primaries (#2, 3, 11) were located in the submandibular/ floor of mouth, with solid histological component; two lung metastasis from parotid primary (#10, 15); and #1, 4, 5, 6, 9, 12, 14, 8 were patients with tumors arising in various locations, with cribriform and tubular patterns, excepting for one case with solid pattern (#9). This patient died of disease while the other patients in these groups are alive. The two patients (#13, 16) in group 3 had ACC solid type which arose in maxilla/hard palate, and died of disease, (see table 3, fig. 4). No stronger correlations with clinical and pathological parameters were noticed for the rest of hyper- and hypomethylated genes.

DISCUSSION

Our study identifies a limited number of differentially methylated gene regions in ACC (32 hypermethylated, and 7 hypomethylated). Several of the affected genes were previously reported to be methylated in cancer, and of known biological functions in tumor formation or promotion.

Some known targets of DNA methylation in cancer were also identified in our study, including the homeobox genes EN1 methylated in colorectal cancer and astrocytomas [7, 8], MEIS1 linked to acute myeloid leukemias [9], metabolic enzyme EPHX3 associated with prostate cancer [10], transcription factor FOXE1 linked to squamous cell carcinoma [11], breast cancer associated gene TFAP2C, and apoptotic activator BCL2L11 methylated in haematological and epithelial cancers[12].

Of special interest are these genes that may play an important role in ACC in salivary gland and were found here to be methylated for the first time, like apoptosis activator PITX1, Wnt/β-Catenin pathway activator FOXL1, and breast cancer associated gene NR2F2.

A pathway analysis of all the genes we found differentially methylated in ACC (34 hypermethylated and 7 hypomethylated genes) using the computer program Ingenuity Pathways Analysis (Ingenuity Systems) did not yield any conclusive or specific pathway results. We assume that DNA methylation results alone do not provide sufficient data to identify the exact biological pathways or gene-networks disrupted in cancer, and thus need support data from other analysis, either by comparison to specific DNA-methylation pathway data bases or by gene expression profiling.

The overall patterns of methylated gene regions were very similar between all tumors tested here, particularly the predominance of methylated genes regulating the expression of genes involved in development and differentiation, due to the large fraction of transcription factors. In detail, we observed significant hypermethylations in regions around genes encoding the transcription factors: EN1, FOXE1, GBX2, FOXL1, TBX4, MEIS1, LBX2, NR2F2, POU3F3, IRX3, TFAP2C, NKX2-4, PITX1, NKX2-5.

EN1 (engrailed homeobox 1) is known to play an important role in the development of CNS. Epigenetic suppression of EN1 is common to most colorectal cancers [7] and in astrocytomas [8]. Methylated EN1-CpG island DNA might be used as biomarker of neoplastic disease [7]. FOXE1 (TTF2, thyroid transcription factor 2) is one of the main factors of development (morphogenesis) of the thyroid gland. FOXE1 plays a crucial role in thyroid cancer [13], and in the development of cutaneous SCC [11]. FOXL1 is an activator of the Wnt/β-Catenin pathway, which is strongly associated with human cancer when dysregulated [14, 15]. POU3F3 (BRN1) [16] and GBX2 are known to be involved in CNS development, with GBX2 as a direct target of the Wnt signaling pathway [17] contributing to multiple types of cancer [18, 19]. TBX4 has been shown to be involved in developmental processes and breast cancer [20], and MEIS1 homeobox gene is involved in cell differentiation [21] and contributes to acute myeloid leukemia [9, 21]. LBX2 (ladybird homeobox 2), is a transcription factor regulating development of muscle fibers [22], and NR2F2[23], and TFAP2C are genes associated with breast cancer [24]. PITX1 is known to be involved in organ development, and is identified as tumor suppressor, probably due to its function as a direct transcriptional activator of tumor suppressor p53[25]. Downregulation of PITX1 is correlated to gastric carcinogenesis, and PITX1 has been shown to induce expression of TBX4[26]. IRX3, and NKX2-4 regulate neuronal development, and NKX2-5 is involved in the formation and development of heart.

We also identified 13 genes with different functions to be hypermethylated in ACC: MT1H which is involved in cellular processes on binding, storage, and transport of Zn/metal ions

[27]. MT1H is a stress response gene, which was found to be downregulated in colon cancer [28]. EPHX3 (epoxide hydrolase 3, ABHD9), a metabolic enzyme which converts mutagenic epoxides into trans-dihydrodiols for detoxication. EPHX3 promoter methylation is associated with prostate cancer [10]. Membrane metallopeptidase AQPEP (laeverin), which plays a role in protein catabolism, and p53 induced apoptotic activator BCL2L11 (BIM) [29]. Carbohydrate transporter SLC35D3, and G protein-coupled receptor S1PR5. PNLIPRP1, which plays a role in lipid catabolism [30], chloride channel protein CLIC6, and Ras GTPase activator RASAL2. XRN2 which is involved in RNA metabolism is associated with lung cancer [31], and GSTM5 a glutathione transferase member of the mu-class enzymes, involved in detoxification of reactive electrophiles is associated with Barett's adenocarcinoma [32]. Desmoplastic response related gene FNDC1[33], and INSRR, an insulin receptor related kinase, which can activate apoptosis [34]. The functions of the six hypermethylated genes C21orf91, MEGF11, KLHDC7B, SLFN13, FAM176B, C1orf113, and the pseudogene MT1IP are yet unknown.

In our study, significant hypomethylation was identified at regions near the genes of FBXO17 encoding F-box protein 17 involved in ubiquitination and glycoprotein catabolism [35], PHKG1 the only phosphorylase kinase expressed in salivary gland and associated with the regulation of glycogen catabolism [36], LOXL1, lysyl oxidase-like 1 an extracellular matrix protein crosslinking type I collagen and elastin, DOCK1, dedicator of cytokinesis 1 involved in cellular and subcellular polarization, including cell migration and phagocytosis [37], and PARVG (parvin, gamma), a member of the parvin family of focal adhesion proteins, which is involved in actin binding for cell-matrix adhesion. PARVG binds to several integrin-signaling related proteins like α4-integrin inducing cell migration, e. g. cell spreading of leukocytes[38]. Two of the hypomethylated gene regions are associated with the unknown genes C19orf24, C15orf38.

Four CpG island regions, with marked hypermethylation identified by MCAM were validated by pyrosequencing, are associated with EN1, FOXE1, TBX4, and PITX1. The pyrosequencing of their CpG islands showed an overall difference in hypermethylation of 52% +/− 9 between tumor and normal samples (fig. 2), implying that this extend of hypermethylation is sufficient for ACC development. It further implies that this might be the quantity of hypermethylation which has to be blocked by potential DNA methylation inhibitors to achieve a biological or therapeutical effect.

Our clinicopathologic correlations show that the EN1 methylation status correlated with histological grading of tumor, location of tumor and final outcome of patient.

To our knowledge, this is the first time that these genes and their respective 32 hypermethylated and 7 hypomethylated gene regions presented here have been implicated in salivary gland tumorigenesis.

A recent promoter methylation profiling study [39], of 78 salivary tumors (26 benign pleomorphic adenomas, 17 ACC, 18 salivary duct carcinomas and 17 mucoepidermoid carcinomas) showed the most significant methylated tumor type was SDC, while ACC and MEC demonstrated less methylation than SDC.

Our findings are at variance with these findings and this may reflect difference in platforms and/or interpretable factors. Our study identifies certain highly hypermethylated genes with minimal intertumoral variations to represent important targets in ACC.

In conclusion, we used MCAM, a high-throughput technique to detect aberrant DNA methylation in adenoid cystic carcinoma of salivary glands. MCAM is highly specific and sensitive and we present here beside the highly hyper- and hypomethylated genes common

in all ACC tumors analyzed here, the EN1 hypermethylated CpG promoter region as a potential biomarker for ACC in salivary gland tumors which might be extended to clinical studies.

Acknowledgments

The study is supported in part by the NIH National Institute of Dental and Craniofacial Research (NIDCR) and Rare Disease Research (ORDR) Grant Number U01DE019756 (AEN, DB), the Head and Neck SPORE program and The Kenneth D. Muller professorship (AEN), the NCI-CA-16672 grant (AEN) and MDACC start-up funds (DB). The content is solely the responsibility of the authors and does not necessarily represent the official views of the National Cancer Institute or the National Institute of Health.

We thank Dr. Lanlan Shen and Rong He from Department of Leukemia, The University of Texas M. D. Anderson Cancer Center, Houston, Texas for discussions and assistance with the MCAM experiments.

References

1. Takai D, Jones PA. Comprehensive analysis of CpG islands in human chromosomes 21 and 22. Proc Natl Acad Sci U S A. 2002; 99(6):3740–5. [PubMed: 11891299]
2. Toyota M, Ho C, Ahuja N, et al. Identification of differentially methylated sequences in colorectal cancer by methylated CpG island amplification. Cancer Res. 1999; 59(10):2307–12. [PubMed: 10344734]
3. Weinmann AS, Yan PS, Oberley MJ, Huang TH, Farnham PJ. Isolating human transcription factor targets by coupling chromatin immunoprecipitation and CpG island microarray analysis. Genes Dev. 2002; 16(2):235–44. [PubMed: 11799066]
4. Estecio MR, Yan PS, Ibrahim AE, et al. High-throughput methylation profiling by MCA coupled to CpG island microarray. Genome Res. 2007; 17(10):1529–36. [PubMed: 17785535]
5. DeRisi J, Penland L, Brown PO, et al. Use of a cDNA microarray to analyse gene expression patterns in human cancer. Nat Genet. 1996; 14(4):457–60. [PubMed: 8944026]
6. Weber M, Davies JJ, Wittig D, et al. Chromosome-wide and promoter-specific analyses identify sites of differential DNA methylation in normal and transformed human cells. Nat Genet. 2005; 37(8):853–62. [PubMed: 16007088]
7. Mayor R, Casadome L, Azuara D, et al. Long-range epigenetic silencing at 2q14.2 affects most human colorectal cancers and may have application as a non-invasive biomarker of disease. Br J Cancer. 2009; 100(10):1534–9. [PubMed: 19384295]
8. Wu X, Rauch TA, Zhong X, et al. CpG island hypermethylation in human astrocytomas. Cancer Res. 2010; 70(7):2718–27. [PubMed: 20233874]
9. Lasa A, Carnicer MJ, Aventin A, et al. MEIS 1 expression is downregulated through promoter hypermethylation in AML1-ETO acute myeloid leukemias. Leukemia. 2004; 18(7):1231–7. [PubMed: 15103390]
10. Cottrell S, Jung K, Kristiansen G, et al. Discovery and validation of 3 novel DNA methylation markers of prostate cancer prognosis. J Urol. 2007; 177(5):1753–8. [PubMed: 17437806]
11. Venza I, Visalli M, Tripodo B, et al. FOXE1 is a target for aberrant methylation in cutaneous squamous cell carcinoma. Br J Dermatol. 2010; 162(5):1093–7. [PubMed: 19845668]
12. Dunwell T, Hesson L, Rauch TA, et al. A genome-wide screen identifies frequently methylated genes in haematological and epithelial cancers. Mol Cancer. 2010; 9:44. [PubMed: 20184741]
13. Landa I, Ruiz-Llorente S, Montero-Conde C, et al. The variant rs1867277 in FOXE1 gene confers thyroid cancer susceptibility through the recruitment of USF1/USF2 transcription factors. PLoS Genet. 2009; 5(9):e1000637. [PubMed: 19730683]
14. Myatt SS, Lam EW. The emerging roles of forkhead box (Fox) proteins in cancer. Nat Rev Cancer. 2007; 7(11):847–59. [PubMed: 17943136]
15. Perreault N, Katz JP, Sackett SD, Kaestner KH. Foxl1 controls the Wnt/beta-catenin pathway by modulating the expression of proteoglycans in the gut. J Biol Chem. 2001; 276(46):43328–33. [PubMed: 11555641]

16. Mutai H, Nagashima R, Sugitani Y, Noda T, Fujii M, Matsunaga T. Expression of Pou3f3/Brn-1 and its genomic methylation in developing auditory epithelium. Dev Neurobiol. 2009; 69(14):913–30. [PubMed: 19743445]

17. Li B, Kuriyama S, Moreno M, Mayor R. The posteriorizing gene Gbx2 is a direct target of Wnt signalling and the earliest factor in neural crest induction. Development. 2009; 136(19):3267–78. [PubMed: 19736322]

18. Glinsky GV, Berezovska O, Glinskii AB. Microarray analysis identifies a death-from-cancer signature predicting therapy failure in patients with multiple types of cancer. J Clin Invest. 2005; 115(6):1503–21. [PubMed: 15931389]

19. Tong WG, Wierda WG, Lin E, et al. Genome-wide DNA methylation profiling of chronic lymphocytic leukemia allows identification of epigenetically repressed molecular pathways with clinical impact. Epigenetics. 2010; 5(6)

20. Kelemen LE, Wang X, Fredericksen ZS, et al. Genetic variation in the chromosome 17q23 amplicon and breast cancer risk. Cancer Epidemiol Biomarkers Prev. 2009; 18(6):1864–8. [PubMed: 19454617]

21. Ji H, Ehrlich LI, Seita J, et al. Comprehensive methylome map of lineage commitment from haematopoietic progenitors. Nature. 2010

22. Ochi H, Westerfield M. Lbx2 regulates formation of myofibrils. BMC Dev Biol. 2009; 9:13. [PubMed: 19216761]

23. Nakshatri H, Mendonca MS, Bhat-Nakshatri P, Patel NM, Goulet RJ Jr, Cornetta K. The orphan receptor COUP-TFII regulates G2/M progression of breast cancer cells by modulating the expression/activity of p21(WAF1/CIP1), cyclin D1, and cdk2. Biochem Biophys Res Commun. 2000; 270(3):1144–53. [PubMed: 10772965]

24. Woodfield GW, Chen Y, Bair TB, Domann FE, Weigel RJ. Identification of primary gene targets of TFAP2C in hormone responsive breast carcinoma cells. Genes Chromosomes Cancer. 2010

25. Liu DX, Lobie PE. Transcriptional activation of p53 by Pitx1. Cell Death Differ. 2007; 14(11): 1893–907. [PubMed: 17762884]

26. Logan M, Tabin CJ. Role of Pitx1 upstream of Tbx4 in specification of hindlimb identity. Science. 1999; 283(5408):1736–9. [PubMed: 10073939]

27. Bigagli E, Luceri C, Bernardini S, Dei A, Dolara P. Extremely low copper concentrations affect gene expression profiles of human prostate epithelial cell lines. Chem Biol Interact. 2010

28. Wilson AJ, Chueh AC, Togel L, et al. Apoptotic sensitivity of colon cancer cells to histone deacetylase inhibitors is mediated by an Sp1/Sp3-activated transcriptional program involving immediate-early gene induction. Cancer Res. 2010; 70(2):609–20. [PubMed: 20068171]

29. Han J, Goldstein LA, Hou W, Gastman BR, Rabinowich H. Regulation of mitochondrial apoptotic events by p53-mediated disruption of complexes between antiapoptotic Bcl-2 members and Bim. J Biol Chem. 2010; 285(29):22473–83. [PubMed: 20404322]

30. Lowe ME. The triglyceride lipases of the pancreas. J Lipid Res. 2002; 43(12):2007–16. [PubMed: 12454260]

31. Lu Y, Liu P, James M, et al. Genetic variants cis-regulating Xrn2 expression contribute to the risk of spontaneous lung tumor. Oncogene. 2010; 29(7):1041–9. [PubMed: 19915612]

32. Peng DF, Razvi M, Chen H, et al. DNA hypermethylation regulates the expression of members of the Mu-class glutathione S-transferases and glutathione peroxidases in Barrett's adenocarcinoma. Gut. 2009; 58(1):5–15. [PubMed: 18664505]

33. Anderegg U, Breitschwerdt K, Kohler MJ, et al. MEL4B3, a novel mRNA is induced in skin tumors and regulated by TGF-beta and pro-inflammatory cytokines. Exp Dermatol. 2005; 14(9): 709–18. [PubMed: 16098131]

34. Weber A, Huesken C, Bergmann E, Kiess W, Christiansen NM, Christiansen H. Coexpression of insulin receptor-related receptor and insulin-like growth factor 1 receptor correlates with enhanced apoptosis and dedifferentiation in human neuroblastomas. Clin Cancer Res. 2003; 9(15):5683–92. [PubMed: 14654552]

35. Glenn KA, Nelson RF, Wen HM, Mallinger AJ, Paulson HL. Diversity in tissue expression, substrate binding, and SCF complex formation for a lectin family of ubiquitin ligases. J Biol Chem. 2008; 283(19):12717–29. [PubMed: 18203720]

36. Winchester JS, Rouchka EC, Rowland NS, Rice NA. In Silico characterization of phosphorylase kinase: evidence for an alternate intronic polyadenylation site in PHKG1. Mol Genet Metab. 2007; 92(3):234–42. [PubMed: 17692548]

37. Premkumar L, Bobkov AA, Patel M, et al. Structural basis of membrane targeting by the Dock180 family of Rho family guanine exchange factors (Rho-GEFs). J Biol Chem. 2010; 285(17):13211–22. [PubMed: 20167601]

38. Yoshimi R, Yamaji S, Suzuki A, et al. The gamma-parvin-integrin-linked kinase complex is critically involved in leukocyte-substrate interaction. J Immunol. 2006; 176(6):3611–24. [PubMed: 16517730]

39. Durr ML, Mydlarz WK, Shao C, et al. Quantitative methylation profiles for multiple tumor suppressor gene promoters in salivary gland tumors. PLoS One. 2010; 5(5):e10828. [PubMed: 20520817]

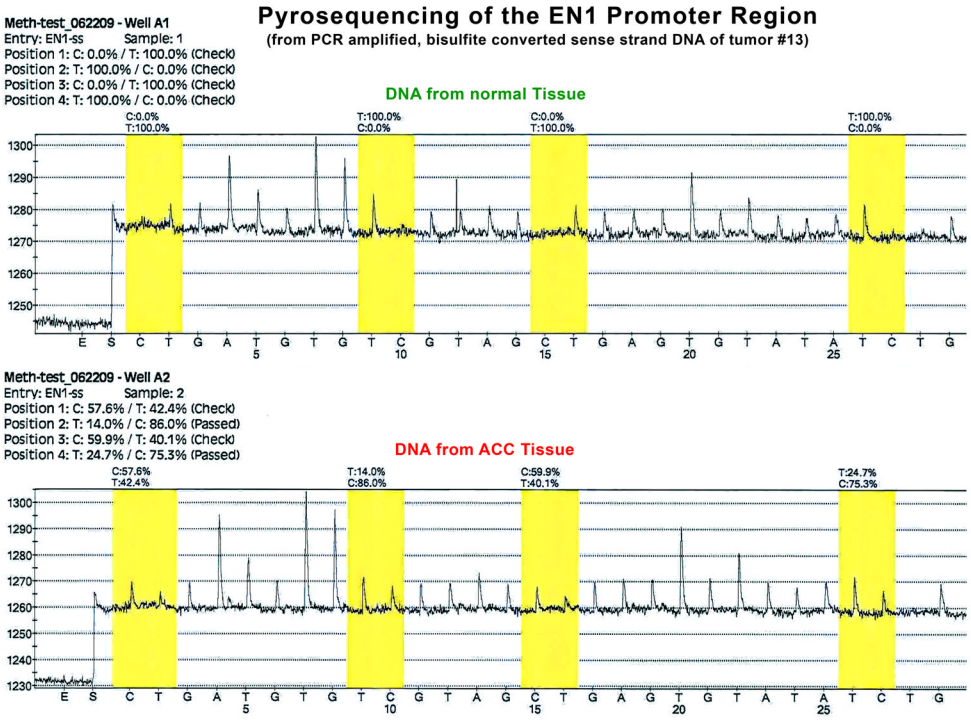

Figure 1.

Pyrosequencing data output for the EN1 promoter region from PCR amplified, bisulfite converted sense strand DNA of tumor 13 (red), and its matching normal tissue (green). Methylation is quantified for each single C of a CpG dinucleotide highlighted in yellow. It is calculated as percent ratio between its methylated form, peak of C and its non-methylated form, peak of T.

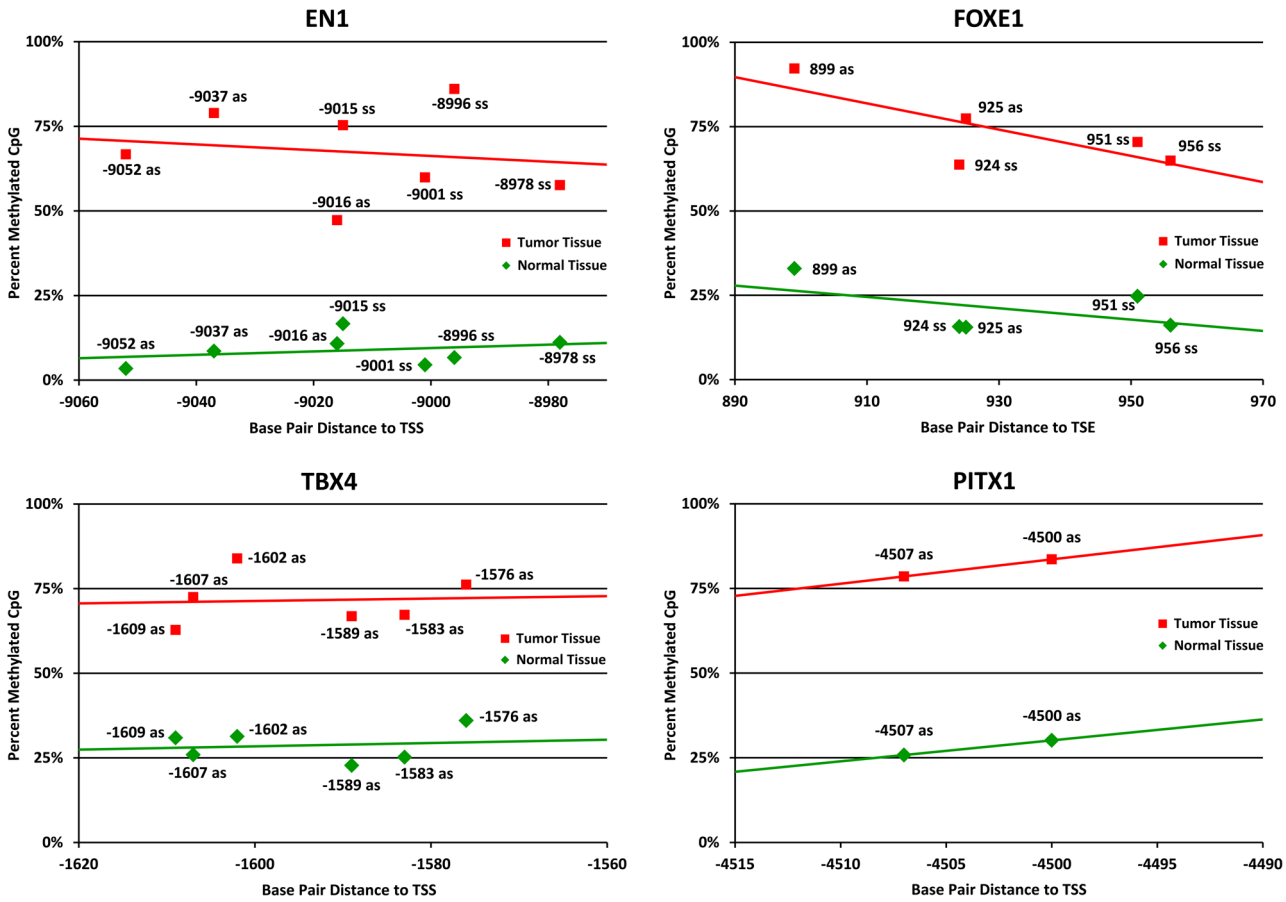

Figure 2.

Pyrosequencing of small areas in CpG islands, associated with the genes EN1, FOXE1, TBX4, and PITX1. The exact locations of methylated cytosines are shown in base-pair distances relative to the transcription start site (TSS) or transcription end (TSE) of the associated gene. Shown is percent methylation for each single CpG from sense strand (ss) and/or anti-sense strand (as) averaged over all tumor patients. Tumor CpG- and the matching normal CpG-methylation is colored in red and green, respectively. A curve fit was performed to determine the average differences of CpG methylation between tumor and normal tissues. For all four gene regions the average methylation difference results to 52 +/ −9 %.

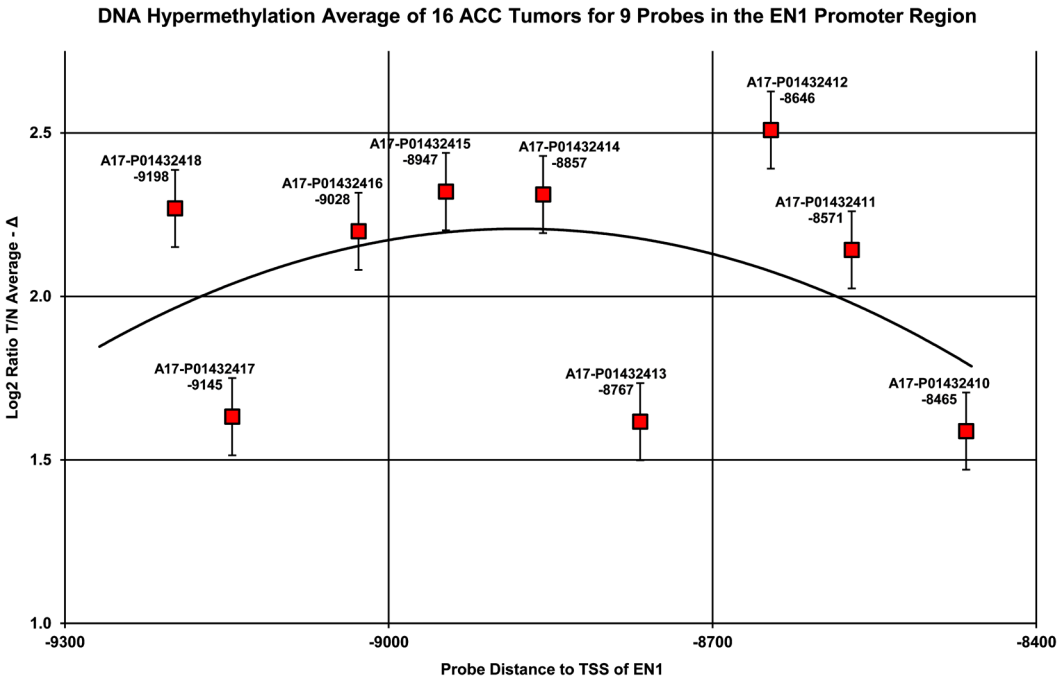

Figure 3.

DNA hypermethylation average over 16 ACC tumors for each of all 9 probes in the EN1 promoter region showing high hypermethylations and high consistency (low standard errors) with MCAM analysis.

A

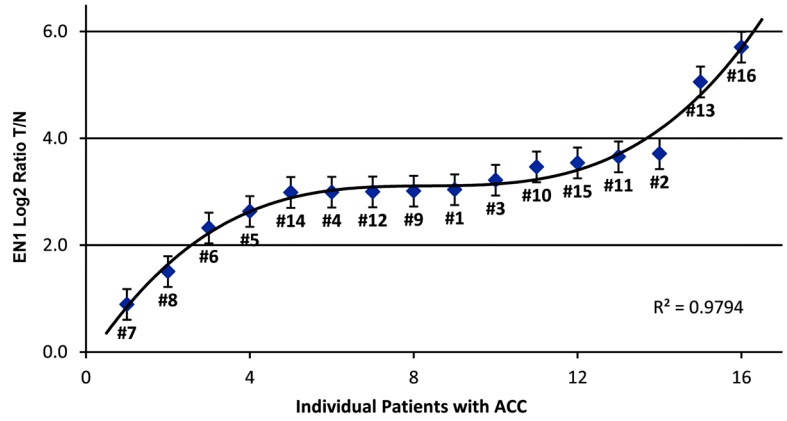

B

Category	Log2 Range	Patient Tumor ID	EN1 Hyper M Log2 Ratio T/N
1	< 2.2	7	0.89
1	< 2.2	8	1.51
2	2.2 to 4.5	6	2.32
2	2.2 to 4.5	5	2.63
2	2.2 to 4.5	14	2.99
2	2.2 to 4.5	4	2.99
2	2.2 to 4.5	12	3.00
2	2.2 to 4.5	9	3.01
2	2.2 to 4.5	1	3.04
2	2.2 to 4.5	3	3.22
2	2.2 to 4.5	10	3.47
2	2.2 to 4.5	15	3.54
2	2.2 to 4.5	11	3.65
2	2.2 to 4.5	2	3.71
3	> 4.5	13	5.06
3	> 4.5	16	5.71

Figure 4.

Correlation of EN1 hypermethylation to individual tumors. A, trendline of hypermethylation of the EN1 promoter region correlated to individual tumors (including standard error bars, and a regression coefficient of 0.9794). B, table with categories of individual tumors correlated to their hypermethylation of the EN1 promoter region.

Table 1

MCAM results: significant hypermethylation average for each CpG island region shown as ranking list and associated genes.

Gene Region Ranking	Hypermethylation Log 2 Ratio T/N Average-Δ	Chr	Description	Gene Symbo	Probe showing highest Hypermethylation (Agilent ID)
1	2.3	chr16	Promoter	MT1H	A_17_P16899559
2	2.1	chr2	Promoter	EN1	A_17_P01432412
3	1.9	chr19	Promoter	EPHX3	A_17_P10894655
4	1.9	chr9	Downstream	FOXE1	A_17_P06839525
5	1.9	chr2	Downstream	GBX2	A_17_P15396508
6	1.8	chr16	Inside	FOXL1	A_17_P16923171
7	1.8	chr5	Inside EX1	LVRN	A_17_P04211235
8	1.8	chr2	Promoter	BCL2L11	A_17_P01402641
9	1.8	chr6	Inside	SLC35D3	A_17_P05106065
10	1.8	chr17	Promoter	TBX4	A_17_P10404890
11	1.7	chr2	Promoter	MEIS1	A_17_P01244855
12	1.7	chr21	Promoter	C21orf91	A_17_P17222457
13	1.7	chr19	Inside EX1	S1PR5	A_17_P10881619
14	1.7	chr15	Promoter	MEGF11	A_17_P09723256
15	1.6	chr2	Promoter	LBX2	A_17_P01281689
16	1.6	chr15	Promoter	NR2F2	A_17_P09853673
17	1.5	chr2	Downstream	POU3F3	A_17_P15295026
18	1.5	chr16	Promoter	MT1IP	A_17_P16899586
19	1.5	chr22	Inside	KLHDC7B	A_17_P17299194
20	1.5	chr10	Promoter	PNLIPRP1	A_17_P07507249
21	1.5	chr21	Promoter	CLIC6	A_17_P11364964
22	1.4	chr1	Promoter	RASAL2	A_17_P15147124
23	1.4	chr16	Promoter	IRX3	A_17_P10024863
24	1.4	chr17	Promoter	SLFN13	A_17_P10300264
25	1.4	chr1	Inside	FAM176B & C1orf113	A_17_P00137866
26	1.4	chr20	Promoter	TFAP2C	A_17_P11230937
27	1.4	chr20	Downstream	XRN2 & NKX2-4	A_17_P11110075
28	1.4	chr1	Inside	GSTM5	A_17_P00450274
29	1.4	chr5	Promoter	PITX1	A_17_P04297797

Gene Region Ranking	Hypermethylation Log 2 Ratio T/N Average-Δ	Chr	Description	Gene Symbo	Probe showing highest Hypermethylation (Agilent ID)
30	1.3	chr6	Inside	FNDC1	A_17_P05207116
31	1.3	chr1	Inside	INSRR	A_17_P00530309
32	1.3	chr5	Inside	NKX2-5	A_17_P04471749

Table 2

MCAM results: significant hypomethylation average for each CpG island region shown as ranking list and associated genes.

Gene Region Ranking	Hypomethylation Log 2 Ratio N/T Average-Δ	Chr	Description	Gene Symbol	Probe showing highest Hypomethylation (Agilent ID)
1	1.5	chr19	Promoter	C19orf24	A_17_P10853237
2	1.4	chr19	Inside	FBXO17	A_17_P10958079
3	1.4	chr15	Promoter	C15orf38	A_17_P09822652
4	1.4	chr7	Promoter	PHKG1	A_17_P05505786
5	1.4	chr15	Inside	LOXL1	A_17_P09758067
6	1.3	chr10	Inside	DOCK1	A_17_P07558245
7	1.3	chr22	Inside	PARVG	A_17_P11522679

Table 3

Clinical Follow-Up of adenoid cystic carcinoma in salivary gland.

#	Age	Sex	Size [cm]	Site	Histology Type	Perineural Invasion	Type of Surgery	Post-Operative		Follow-Up		EN1 Hyper M Log 2 Ratio T/N
								X-RT	Chemo	Recurrence	Metastasis	
1	48	M	5.0	BOT	Cribriform	+	BOT and partial pharyngectomy	yes	no	no	no	3.04
2	45	F	2.2	FOM	Cribriform	−	submandibular and FOM resection	yes	no	no	no	3.71
3	69	F	2.0	Subman-dibular	Cribriform	−	submandibular and neck dissection	yes	no	no	no	3.22
4	64	F	5.0	Pharynx	Tubular	+ +	pharyngectomy	yes	no	concurrent lung primary adenoca	no	2.99
5	49	F	1.0	BOT	Tubular	+	BOT	no	no	no	no	2.63
6	56	F	1.0	Retromolar	Cribriform	+ +	parotidectomy	yes	no	extensive loco-regional recurrence	no	2.32
7	41	M	1.2	Parotid	Cribriform	−	parotid bed (2001 PA)	yes	no	no	no	0.89
8	66	M	2.0	Lip	Cribriform	+	lip resection	yes	no	no	no	1.51
9	65	M	6.5	Maxilla	Solid	+ +	maxillectomy	yes	yes	deceased	liver and lung metastases	3.01
10	57	F	4.5	Lung Metastasis	Cribriform	N/A	parotidectomy	yes	no	no	lung metastases	3.47
11	76	M	3.0	FOM	Solid	+ +	FOM resection	no	no	local recurrence	no	3.65
12	45	F	2.5	Maxilla	Cribriform	+ +	maxillectomy	yes	no	no	lung metastases	3.00
13	64	M	4.0	Palate	Solid	+ +	maxillectomy	yes	yes	deceased	bone and liver metastasis	5.06
14	85	F	3.0	Maxilla	Solid	+	total palatectomy	yes	no	no local recurrence	no	2.99
15	37	M	2.0	Parotid	Cribriform	+	total parotidectomy	yes	yes	stable disease	lung metastasis	3.54
16	56	F	3.0	Maxilla	Solid	+	partial maxillectomy and total palatectomy	yes	no	deceased	no	5.71